NASA TECHNICAL NOTE

NASA TN D-4592

c. 1

NASA TN D-4592

TECH LIBRARY KAFB, NM

0131049

LOAN COPY: RETURN TO
AFWL (WLIL-2)
KIRTLAND AFB, N MEX

CAVITATING PERFORMANCE OF TWO LOW-AREA-RATIO WATER JET PUMPS HAVING THROAT LENGTHS OF 7.25 DIAMETERS

by Nelson L. Sanger

Lewis Research Center
Cleveland, Ohio

Received
8 JUN 1968

NATIONAL AERONAUTICS AND SPACE ADMINISTRATION • WASHINGTON, D. C. • MAY 1968

TECH LIBRARY KAFB, NM

0131049

NASA TN D-4592

CAVITATING PERFORMANCE OF TWO LOW-AREA-RATIO WATER JET PUMPS HAVING THROAT LENGTHS OF 7.25 DIAMETERS

By Nelson L. Sanger

Lewis Research Center
Cleveland, Ohio

NATIONAL AERONAUTICS AND SPACE ADMINISTRATION

For sale by the Clearinghouse for Federal Scientific and Technical Information
Springfield, Virginia 22151 – CFSTI price $3.00

CONTENTS

	Page
SUMMARY	1
INTRODUCTION	2
MECHANISM AND ANALYSIS OF CAVITATION	3
Mechanism of Cavitation in Jet Pump Flow	3
Analysis	4
Previously reported analyses	5
Present analysis	6
APPARATUS AND PROCEDURE	7
Apparatus	7
Experimental Procedure	9
Cavitation Criteria	9
Air content	9
Incipience	10
Time delay effect	10
RESULTS AND DISCUSSION	10
Noncavitating Performance	10
Overall Cavitating Performance	12
Effect of Flow ratio	15
Effect of nozzle spacing	16
Photographs of cavitation	18
Prediction Parameters	21
Cavitation prediction parameter	21
Effect of nozzle spacing	22
Comparison with previously reported results	22
Alternate cavitation prediction parameter	24
SUMMARY OF RESULTS	26
APPENDIXES	
A - SYMBOLS	28
B - DEVELOPMENT OF JET PUMP CAVITATION ANALYSES	30
I. Gosline and O'Brien Analysis	30
II. Rouse Parameter	32
III. Bonnington Modified Rouse Parameter	32
IV. Cavitation Prediction Parameter	33
V. Alternate Cavitation Prediction Parameter	35
REFERENCES	36

CAVITATING PERFORMANCE OF TWO LOW-AREA-RATIO WATER JET PUMPS HAVING THROAT LENGTHS OF 7.25 DIAMETERS

by Nelson L. Sanger

Lewis Research Center

SUMMARY

Cavitation performance (total headrise as a function of pumped fluid inlet pressure) of two jet pumps was evaluated in a closed-loop facility using room-temperature, deaerated water. Objectives of the investigation were to study the cavitation performance of jet pumps having low ratios of nozzle to throat area and to examine methods of cavitation prediction in jet pumps.

Experimental performance was obtained with two nozzles operated separately in one test section. The test section had a throat diameter of 1.35 inches (3.43 cm), a throat length of 7.25 diameters, and a diffuser included angle of $8^{\circ}6'$ (0.141 rad). The nozzles had exit diameters corresponding to nozzle- to throat-area ratios of 0.066 and 0.197. Each nozzle was operated at three spacings of the nozzle exit from the throat entrance. At each nozzle spacing, tests were conducted at four values of seconary- to primary-flow ratio, while secondary (pumped fluid) inlet pressure was varied.

Extensive amounts of cavitation were observed before performance was affected. However, when the head ratio deteriorated, it did so quite sharply. At a fixed nozzle position, an increase in secondary- to primary-flow ratio resulted in a greater required secondary fluid inlet pressure in order to suppress cavitation. At any fixed flow ratio, less secondary fluid inlet pressure was required to suppress cavitation as the nozzle was retracted from the throat entrance.

For the test section considered in this investigation, a nozzle spacing of approximately 1 throat diameter best satisfied the two major performance requirements of high efficiency and cavitation resistance. The design of the secondary inlet region was important to jet pump cavitation performance. Smooth hydrodynamic streamlining of this region and a thin nozzle wall at the nozzle exit would reduce cavitation susceptibility.

Two related parameters are proposed which are useful in predicting the conditions at which total headrise deteriorates because of cavitation.

INTRODUCTION

Future space vehicles will require large quantities of electric power. One means of meeting these requirements is through the use of a Rankine cycle system having a liquid metal as the working fluid. Jet pumps have several possible applications in such systems (refs. 1 to 3). In order to achieve high system efficiencies, high boiler temperatures and pressures and low radiator temperatures and pressures are necessary. This combination, in addition to a requirement for low power absorption by the jet pump, results in jet pumps having low ratios of nozzle exit area to throat area (jet pump area ratio R). Jet pumps having low area ratios require a relatively low quantity of flow to be recirculated to the nozzle by the main-stage pump (primary or high pressure "booster" flow Q_1), thus keeping the main-stage-pump size, weight, and power requirements low.

In a previous report, jet pump design considerations were explored, both analytically and experimentally, for the case of noncavitating operation (ref. 3). However, in Rankine cycle space systems, cavitation in the pumps represents a serious problem. Radiator condensate pumps and boiler recirculation pumps must handle fluid quite near saturation temperature. Cavitation can be suppressed by subcooling the fluid. But utilizing subcooling as the only method of cavitation supression results in an unacceptable system weight penalty due to the need for additional radiator-condenser sections. One solution to this problem is the use of a limited amount of subcooling and a cavitation-resistant auxiliary pump to boost inlet pressure to the main-stage pump. If a jet pump is used as an auxiliary unit, or in certain applications as a main-stage unit, a knowledge of jet pump cavitation performance will be necessary to optimize system weight and performance.

No single method of predicting the cavitation-imposed operating limits of jet pumps has yet been agreed on. The mechanism of cavitation in a jet pump is closely related to the turbulent mixing process. This process is not yet fully understood, particularly for the case of a ducted jet.

Jet pump cavitation was first discussed in reference 4 for the condition at which cavitation caused total headrise to drop off. Limiting secondary (pumped) flow Q_2 was predicted by application of the one-dimensional energy and continuity relations. With room-temperature water as the test fluid, a general but uneven correlation between theory and experiment was achieved. Rouse (ref. 5), working also with room-temperature water, investigated cavitation produced by a submerged jet ejecting into a large tank of quiescent water. He was able to correlate audible incipient cavitation at different flow rates by using a conventional cavitation number. In reference 6, Bonnington attempted to modify the Rouse parameter to apply to the ducted flow of a jet pump. His experimental data, which corresponded to the condition of total headrise dropoff and not incipience, did not correlate with the modified Rouse parameter. Contrary to these results, experimental data published by Mueller (ref. 7), also for the condition of total headrise dropoff, agreed

with the modified Rouse parameter. Other cavitation prediction parameters have been suggested (refs. 8 and 9) but have not been used widely. A summary presentation of these parameters is given in reference 7.

The present investigation was conducted to study the cavitation performance of jet pumps having low area ratios and to examine methods of cavitation prediction in jet pumps further. Specifically, cavitation performance was investigated in terms of the characteristics of the jet pump total headrise at constant values of secondary- to primary-flow ratio M as the inlet pressure of the secondary fluid Q_2 was reduced. Although the conditions at which total headrise deteriorated were of principal interest, performance conditions were obtained for all stages of cavitation.

Experimental performance at two area ratios, $R = 0.197$ and 0.066, was recorded by operating two nozzles separately in one test section. Three different spacings of the nozzle exit upstream from the throat entrance were investigated for each area ratio. Deaerated, room-temperature tap water was used as the test fluid. The acrylic plastic test section was constructed with a circular bell-mouth entry, a constant diameter throat having a length of 7.25 diameters, and a diffuser of $8^{\circ}6'$ (0.141 rad) included angle. Operating conditions included primary flow rates of 33 and 75 gallons per minute (2.08 and 4.74×10^{-3} m^3/sec), secondary flow rates of 85 to 150 gallons per minute (5.36 to 9.47×10^{-3} m^3/sec), and secondary inlet pressures of 4 to 25 pounds per square inch absolute (2.76 to 17.2×10^4 N/m^2 abs).

MECHANISM AND ANALYSIS OF CAVITATION

Mechanism of Cavitation in Jet Pump Flow

To interpret experimental results accurately requires some knowledge of the mechanism of cavitation inception and development in a jet pump. As defined by Holl and Wislicenus (ref. 10), "The term cavitation shall denote the formation of vapor or gas filled voids within a liquid under the influence of local pressure reductions produced by dynamic action." The model of cavitation inception that has gained the widest acceptance is the nuclei theory (ref. 11). Theoretical analyses (ref. 12) predict that a pure liquid can sustain considerable tensile stress before fracturing. Experimental investigations of highly purified and deaerated water (refs. 13 and 14) have confirmed the existence of liquid tension, but of a magnitude less than theoretically predicted. Other investigations (refs. 15 and 16), which used unmodified water, have reported even smaller tensions, but still of the order of several pounds per square inch (N/m^2).

This inability of a liquid to sustain theoretically predicted tensions has been attributed to the presence of "weak spots" or nuclei. A liquid under tension is metastable,

and nuclei of sufficient size provide the required disturbance to produce instability. The nuclei have been hypothesized as consisting of small volumes of undissolved gas present in crevices of the boundary material and in crevices of microscopic dust particles present in the free stream. A nucleus of sufficient size exposed to a pressure lower than a critical value grows rapidly. Exposure need only be for short time intervals (e.g., 10 μsec for a spherical bubble 0.001 in. (0.0025 cm) in diameter, ref. 17) to initiate the process.

For the case of unseparated flow, in which the minimum pressure occurs at the boundary, it has generally been possible, with the exception of certain scale effects (ref. 10), to predict cavitation inception with the aid of the conventional cavitation number. The use of fluid vapor pressure as critical pressure has proved successful for most engineering applications (ref. 11). In separated flow and shear flow, however, the minimum pressure does not occur at the boundary but in the shear layer, and experimental results have had to be relied on as the chief source of information. In reference 18, the turbulence level in boundary-layer flow was related to cavitation inception. Incipient cavitation was observed to occur in the center of the boundary layer. This suggests that nuclei were being transported from the wall to the center of the vortical eddies in the turbulent boundary layer.

Flow in a jet pump is of the shear type. The primary and secondary fluids are separated by a shear or mixing layer composed of many small turbulent eddies. The experiments of reference 4 confirmed the existence of low local pressures related to turbulence in jet mixing layers. Cavitation occurs in the mixing layer, and it is likely that the mechanism of occurrence is identical to that observed in turbulent boundary layers, with the exception of the source of the nuclei. In the experiments of reference 18, the source of nuclei was the wall next to the boundary layer. In jet pumps, there are two likely sources: free-stream nuclei, and nuclei transported by the boundary layer flowing over the primary nozzle surfaces.

Analysis

Because the flow in a jet pump is a shear flow, cavitation inception conditions are not readily predicted. Not enough is presently known of the relation between the minimum local pressures in the mixing layer and important jet pump flow parameters. In jet pump flow, however, cavitation inception is not of primary interest. The conditions at which jet pump total headrise deteriorates as a result of cavitation are the more critical conditions from the standpoint of design and application.

The nomenclature used in the following discussion of analyses is established in figure 1 and appendix A. The primary fluid Q_1 is pressurized by an independent source

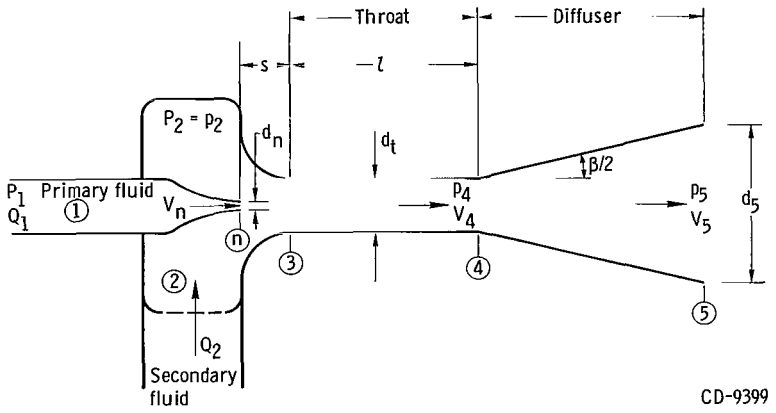

Figure 1. - Schematic representation of jet pump.

and is accelerated to high velocity in the primary nozzle. In a Rankine cycle system, in which the jet pump is used as an auxiliary pump to the condensate pump, the primary fluid is the recirculated fluid, sometimes referred to as the "booster" flow. The secondary fluid is the pumped fluid and is entrained by and mixed with the high-velocity primary fluid in the constant-diameter throat section. The mixed fluids pass through a diffuser which converts a part of the velocity head to static pressure. In a Rankine cycle system application, the secondary flow rate is equivalent to the flow rate through the main cycle.

Jet pump performance is commonly expressed by the following parameters: the secondary- to primary-flow ratio, $M = Q_2/Q_1$; the head ratio, $N = (H_5 - H_2)/(H_1 - H_5)$; and the nozzle- to throat-area ratio, $R = A_n/A_t$.

Previously reported analyses. - The analysis of reference 4 did not attempt to account for the character of the mixing process nor conditions at cavitation inception. The analysis is presented in appendix B section I by using nomenclature convenient to this report. Application of the energy and continuity relations to the secondary fluid results in an expression for secondary flow rate. The assumption was made that, at the point of total headrise breakdown due to cavitation, the pressure in the plane of the primary nozzle was equivalent to vapor pressure at the inlet temperature of the secondary fluid. The resulting expression for Q_2 is the maximum attainable secondary flow rate.

In reference 5, Rouse conducted an experimental investigation of cavitation inception in a free jet, using water as the test fluid. The parameter employed was the conventional cavitation number (appendix B section II) in which the correlating pressure was the pressure in the field surrounding the nozzle p_F, and the reference velocity was the nozzle exit velocity. Because a free jet was investigated, the pressure p_F remained constant

throughout the mixing region, and the "secondary" fluid was entrained from the rest. A value of the cavitation parameter $\sigma_R = 0.6$ correlated audible incipient cavitation over a range of flow rates. Rouse recognized the influence of turbulence in the mixing zone on the mechanism of cavitation. But he also pointed out the difficulties involved in constructing an accurate prediction index based on turbulence parameters (e.g., the nonisotropic character of turbulence in the mixing zone, the experimental problem of measuring the parameters, and the question of whether it is the rms or average negative peak pressure that is significant in the process).

A modification of the Rouse parameter was introduced by Bonnington (ref. 6) to account for the influence of the bounding walls on the jet in a jet pump (appendix B section III). It is debatable whether the physics of the mixing process permit such a facile transformation from the case of free to ducted jets. It is even more questionable whether the value of $\sigma_R = 0.6$, determined for the case of incipient cavitation in a free jet, can be properly used to predict the point of cavitation-induced head breakdown in a jet pump. The experimental results of reference 6 did not correlate with the modified parameter but did produce a regular correlation with the velocity ratio V_3/V_n. However, in reference 7, data were presented (for the point of performance breakdown) which correlated closely with the modified Rouse parameter. There was thus a direct contradiction between the experimental results of reference 6 and reference 7. The differences and the reasons for them are discussed in the section Cavitation prediction parameter (p. 21).

Present analysis. - In appendix B section IV, a parameter is developed which brings together the two analyses set forth by Gosline and O'Brien (ref. 4) and by Bonnington (ref. 6). The energy and continuity relations are applied to the secondary fluid, and the resulting expressions are made dimensionless by dividing by the velocity head of the primary fluid at the nozzle exit. It is assumed that at the condition of total headrise breakdown, the pressure in the plane of the nozzle exit p_3 will be equal to vapor pressure. The resulting expression at the point of total headrise deterioration

$$\omega = \frac{P_2 - p_v}{\frac{\gamma V_n^2}{2g}} = \left(\frac{V_3}{V_n}\right)^2 (1 + K_s) \tag{B7}$$

is essentially the expression that Mueller noted would correlate Bonnington's data. It is also closely related to the parameter used by Gosline and O'Brien.

APPARATUS AND PROCEDURE

Apparatus

The facility used in these tests was the same as that described in reference 3. A schematic diagram of the facility is shown in figure 2. Working fluid was deaerated tap water continuously filtered to remove particles larger than 25 microns. System pressure was varied by pressurization of two bladder-type accumulators. The pressurizing medium (air) was therefore never in contact with the working fluid, and the air content was maintained at approximately 3 parts per million.

The test pump was also the same as that used in reference 3. The test section (fig. 3) was fabricated from acrylic plastic to permit visual observation and photographic studies to be made. A 5-inch (12.7-cm) circular radius bell mouth was used as inlet to a constant diameter (1.35 in. (3.43 cm)) throat section having a length of 7.25 throat diameters. The throat was followed by a conical diffuser having an included angle of $8^{\circ}6'$ (0.141 rad) and an outlet- to inlet-area ratio of 7.73. Static pressure taps of 0.020 inch (0.051 cm) in diameter were installed at 18 axial locations: two in the secondary inlet region, nine in the throat, and seven in the diffuser.

Two nozzles were used in conjunction with the test section and are shown in figure 4. Nozzle spacing (distance from nozzle exit to throat entrance) was varied by inserting shims between the nozzle flange and a reference surface on the secondary plenum.

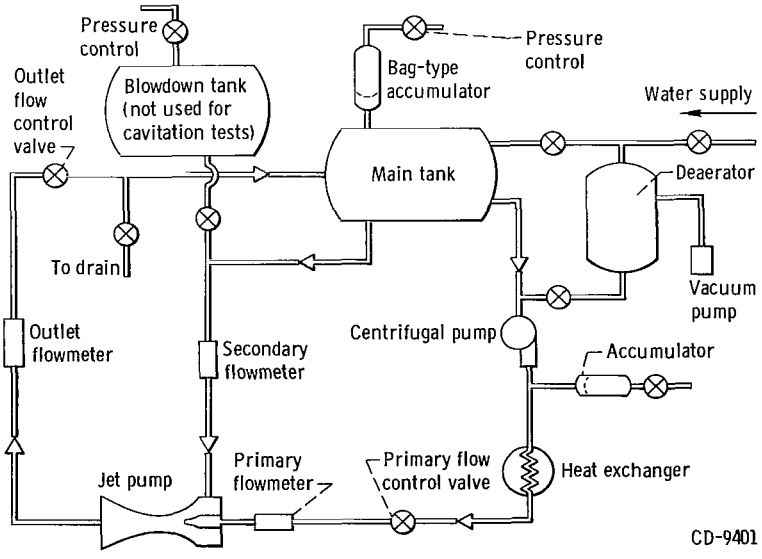

Figure 2. - Schematic drawing of water jet pump test facility.

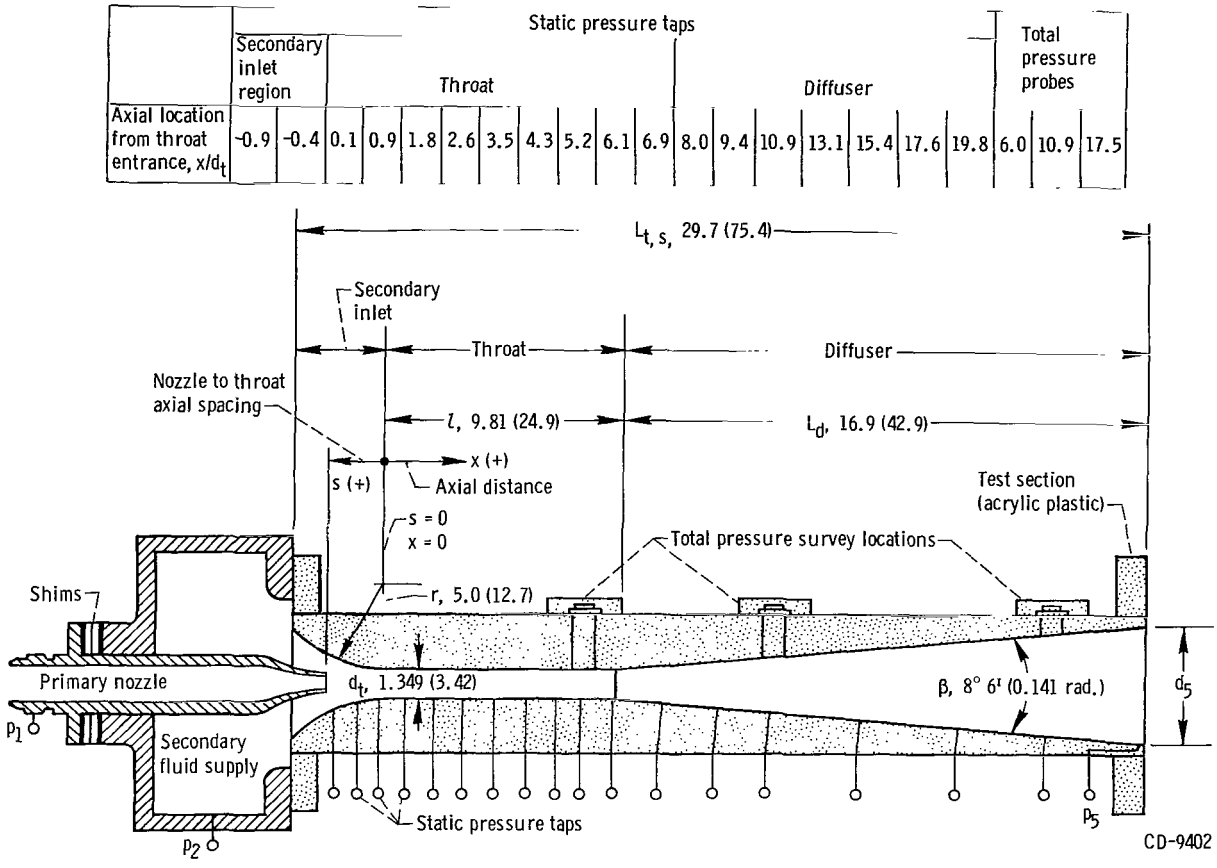

Figure 3. - Schematic diagram of test pump and location of static pressure taps and total pressure probes. Diffuser area ratio, $(d_5/d_t)^2$, 7.73. (All dimensions are in inches (cm).)

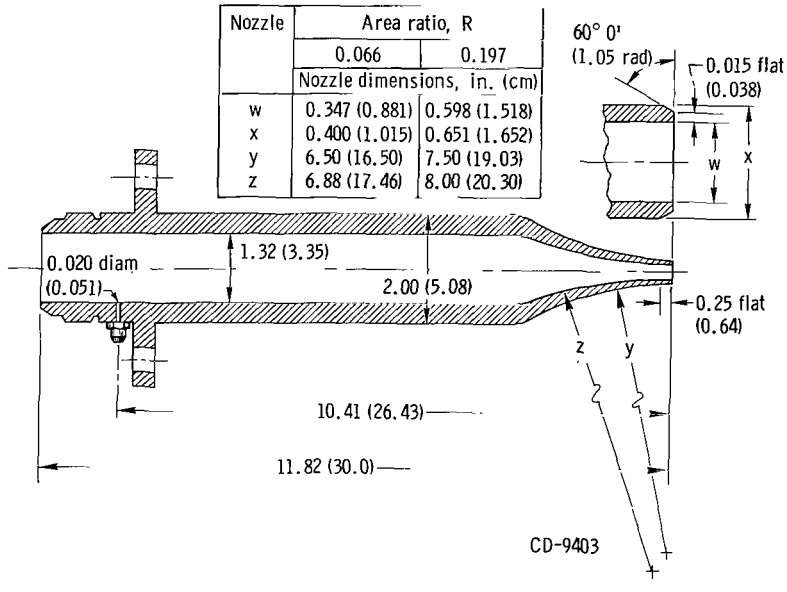

Nozzle	Area ratio, R	
	0.066	0.197
	Nozzle dimensions, in. (cm)	
w	0.347 (0.881)	0.598 (1.518)
x	0.400 (1.015)	0.651 (1.652)
y	6.50 (16.50)	7.50 (19.03)
z	6.88 (17.46)	8.00 (20.30)

Figure 4. - Jet pump primary nozzles. (All dimensions are in inches (cm).)

The primary fluid inlet pressure was read on a Bourdon tube gage. All other pressures used for data reduction were measured on manometers.

Primary and secondary flow rates were measured by turbine flowmeters. The total flow rate was measured by a venturi flowmeter. The venturi-measured flow rate generally agreed within ±2 percent with the sum of the primary and secondary flow rates.

Air content was measured with a Van Slyke Gas Apparatus. Photographs of cavitation were obtained with a 70-millimeter still camera coupled to a flash unit.

The estimated error (instrument and readability combined) of the principal measured variables is listed as follows:

Headrise and static pressures, percent	$< \pm 0.7$
Inlet pressure (primary stream), percent	$< \pm 0.6$
Flow rate, percent:	
Primary stream	$< \pm 1.0$
Secondary stream	$< \pm 2.0$
Temperature, $^{\circ}F$ ($^{\circ}C$)	$< \pm 2$ (± 1.1)

Experimental Procedure

The experimental investigation was conducted with one test section (fig. 3) and two nozzles (fig. 4) having exit diameters corresponding to nozzle- to throat-area ratios of $R = 0.066$ and 0.197. For each area ratio, several values of secondary- to primary-flow ratio were selected which spanned the flow ratio at the best efficiency point.

For a given value of flow ratio M, the jet pump operating characteristic defines a corresponding value of head ratio N. If M is held constant, N will also remain constant as secondary inlet pressure is reduced, until severe cavitation causes either M or N or both to deteriorate. For each selected value of flow ratio, secondary inlet pressure P_2 was reduced in discrete steps until cavitation caused a sharp drop in performance. This procedure was carried out at three nozzle spacings for each area ratio: one at the fully inserted nozzle position, another at about a spacing of 1 throat diameter, and a third at a large spacing.

Cavitation Criteria

Air content. - Several reports noted that decreasing the air content of test water will reduce the number of nuclei having diameters greater than the critical size for inception. This will result in a lower susceptibility to cavitation and will make comparison of results from different test installations difficult. Space electric power systems,

however, will be designed to operate with liquid metals as the working fluid. The gas content of these fluids, particularly in the high-temperature liquid-vapor cycles proposed, will be extremely low. Thus, these conditions were considered to be simulated best in the water system by reducing gas content to the lowest value practicable.

It should be recognized, however, that although the size and number of free undissolved gas bubbles was small, foreign particles up to 25 microns were present. When compared with the size of nuclei required to initiate cavitation, this is not an exceptionally small size.

Incipience. - Cavitation was produced by reducing secondary inlet pressure while maintaining primary and secondary flow rates constant. Principally, it was desired to evaluate the operating conditions for which total headrise deteriorated because of cavitation. Thus, precise determination of conditions of incipience (e.g., questions of audible against visible cavitation) was not stressed. Generally, the condition at which cavitation first became visible was recorded. But there was a generous degree of randomness to these points, and there appeared to be no consistent correlation of them. No attempt was made to define the conditions at which cavitation disappeared by increasing the secondary inlet pressure (cavitation desinence).

Time delay effect. - In references 19 and 20, a cavitation time-delay factor was discussed. Holl and Treaster (ref. 19) observed that, as pressure was decreased, incipient cavitation appeared at a specific pressure only after a finite time had elapsed. Lienhard and Stephenson (ref. 20) related this time delay to a stability phenomenon which controls inception. The time delay was observed during the course of the present jet pump cavitation research. A rapid reduction of inlet pressure to a preselected level resulted, after a delay of several seconds, in the sudden and violent appearance of cavitation. Consequently, when data runs were taken, the inlet pressure was reduced slowly, and system variables were given time (approximately 1/2 to 1 min) to stabilize before data points were recorded.

RESULTS AND DISCUSSION

Noncavitating Performance

Typical noncavitating performance curves from reference 3 are reproduced in figure 5. Jet pump noncavitating performance is commonly presented nondimensionally as head ratio and efficiency as functions of flow ratio. The efficiencies recorded for both area ratios compare quite favorably with efficiencies reported to date in the literature.

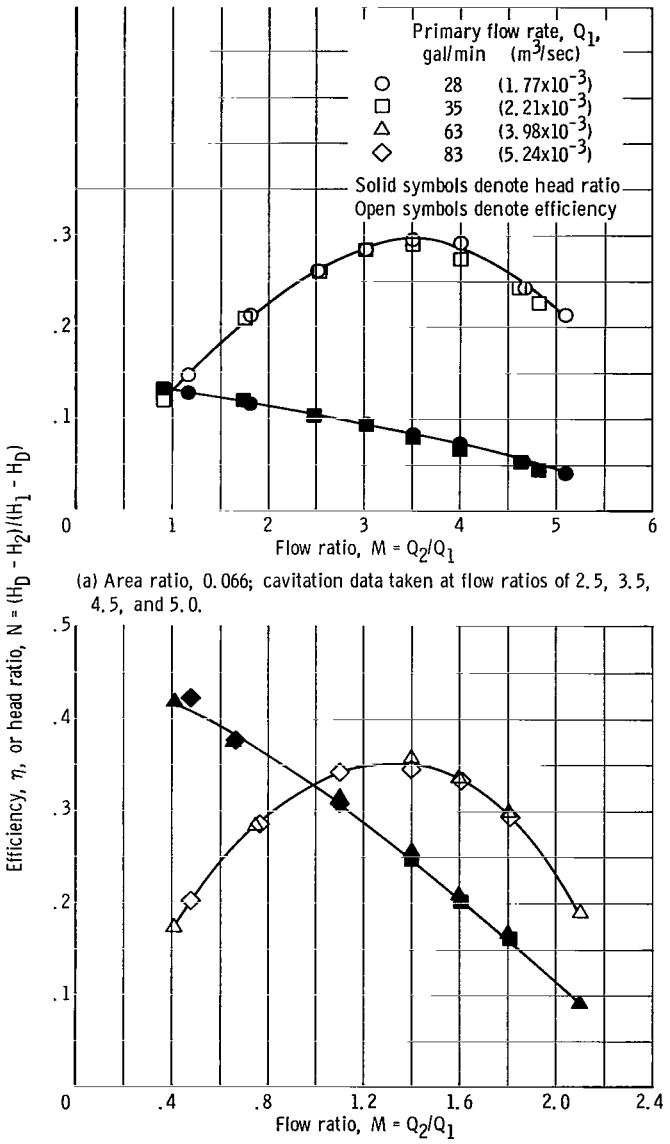

(a) Area ratio, 0.066; cavitation data taken at flow ratios of 2.5, 3.5, 4.5, and 5.0.

(b) Area ratio, 0.197; cavitation data taken at flow ratios of 0.9, 1.3, 1.7, and 2.0.

Figure 5. - Noncavitating jet pump performance for two area ratios. Fully inserted nozzle position; nozzle spacing, 0.

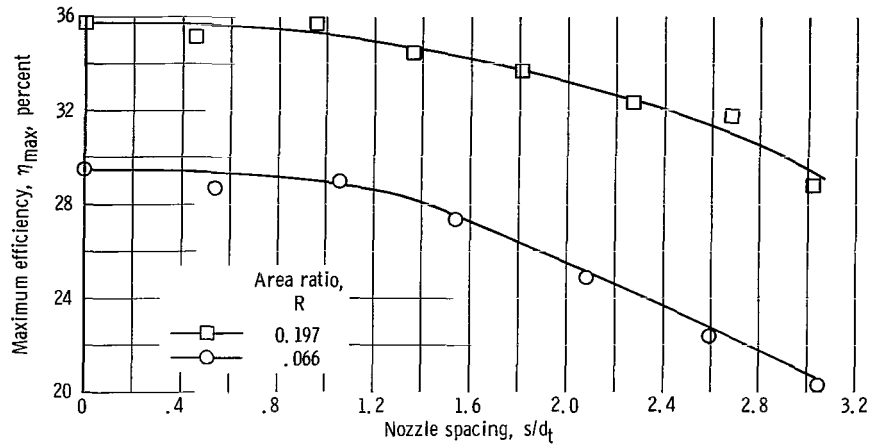

Figure 6. - Noncavitating jet pump performance. Effect of nozzle spacing on maximum efficiency. Cavitation data taken for area ratio of 0.066 at nozzle spacings of 0, 1.05, and 2.58 and for area ratio of 0.197 at nozzle spacings of 0, 0.95, and 2.68.

An important effect investigated in reference 3 was the effect on peak efficiency of the spacing of the nozzle exit from the throat entrance. This effect is summarized in figure 6. For a jet pump having a relatively long throat length (7.25 diam), the most efficient nozzle position was the fully inserted position ($s/d_t = 0$). High values of efficiency were maintained at spacings of up to 1 throat diameter for both area ratios.

Overall Cavitation Performance

Cavitation performance runs were conducted at three nozzle positions for each nozzle- to throat-area ratio. At each nozzle position, characteristic curves of head ratio N against net positive suction head of the secondary fluid $H_{s,v}$ were obtained at four values of secondary- to primary-flow ratio M. The flow ratios chosen were as follows: one corresponding to peak efficiency M_{bep}, one at a flow ratio less than M_{bep}, and two at flow ratios greater than M_{bep}. The values of flow ratio and nozzle position selected for these tests are indicated in the figures.

In figure 7, experimental values of head ratio N are plotted as a function of net positive suction head of the secondary fluid $H_{s,v}$. Three sets of curves, corresponding to three nozzle positions, are shown for each area ratio. Each set of curves was obtained at a constant value of primary flow rate Q_1. The range of flow ratios, therefore, represents a range of secondary flow rates. Furthermore, the values of $H_{s,v}$ at which total headrise deteriorated are applicable only for the flow conditions specified. For the same

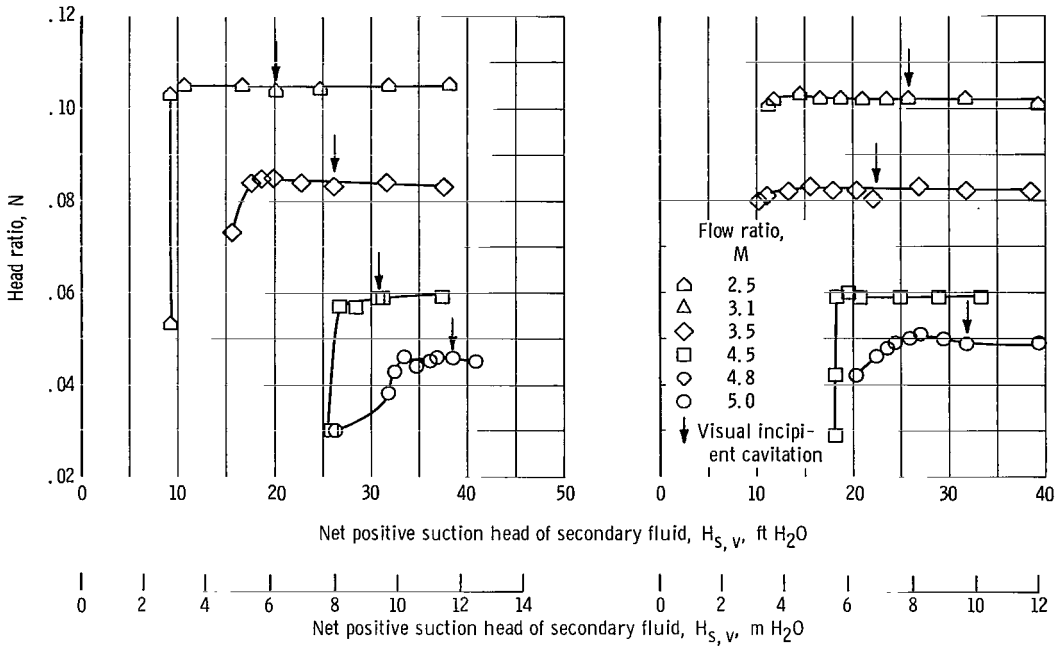

(a-1) Nozzle spacing, 0.

(a-2) Nozzle spacing, 1.05.

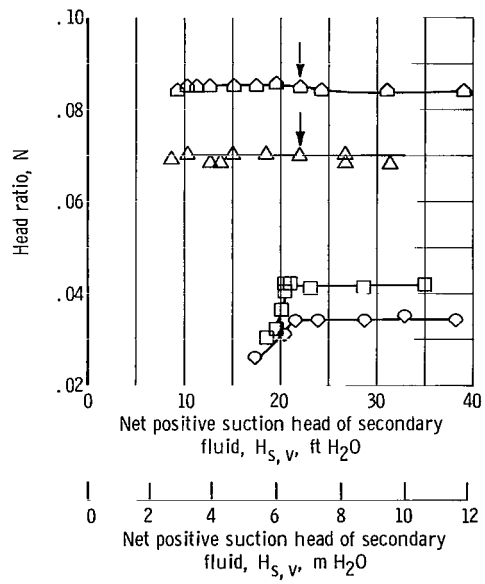

(a-3) Nozzle spacing, 2.58.

(a) Area ratio, 0.066; primary flow rate, 33.0 gallons per minute (2.08×10^{-3} m^3/sec).

Figure 7. - Effect of net positive suction head and flow ratio on jet pump cavitation performance.

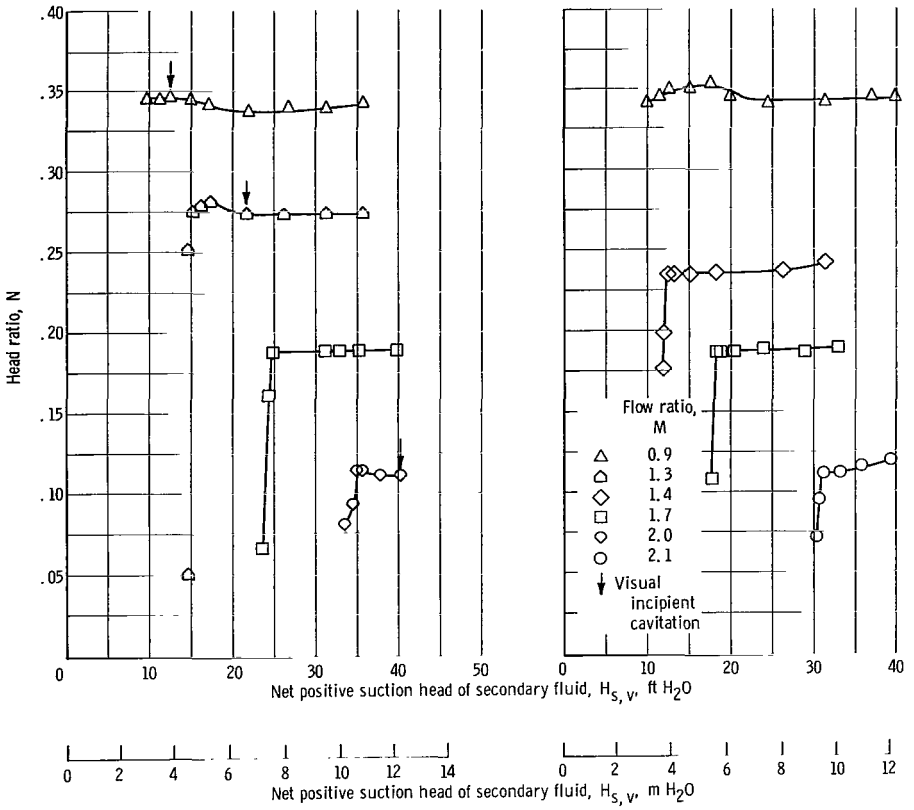

(b-1) Nozzle spacing, 0.

(b-2) Nozzle spacing, 0.95.

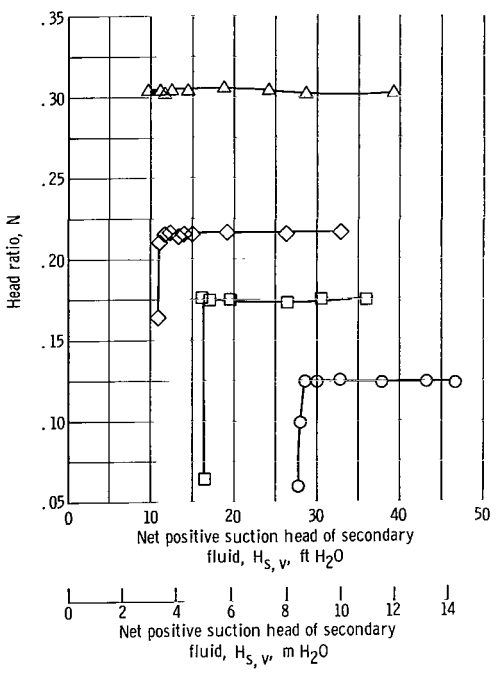

(b-3) Nozzle spacing, 2.68.

(b) Area ratio, 0.197; primary flow rate, 75 gallons per minute (4.74×10^{-3} m^3/sec).

Figure 7. - Concluded.

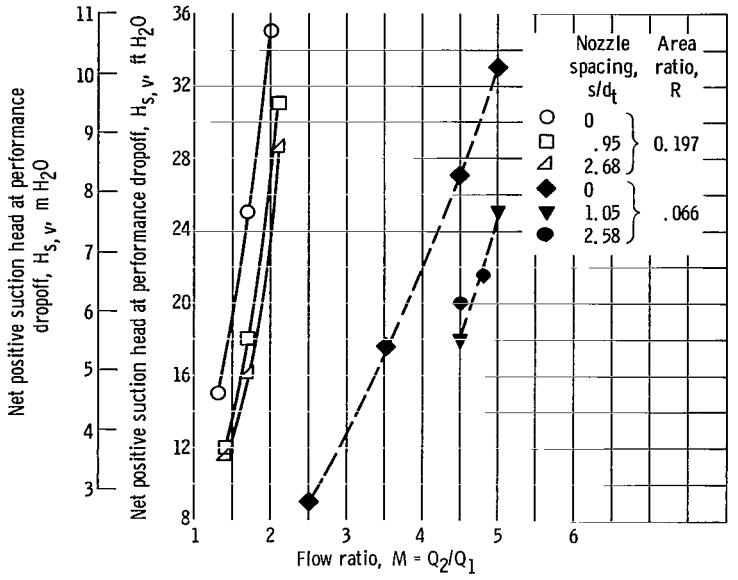

Figure 8. - Effect of flow ratio on required net positive suction head.

secondary- to primary-flow ratio, a higher primary flow rate would result in a performance dropoff at a higher value of $H_{s,v}$. Arrows mark the approximate pressure level at which visual incipience was noted. Incipient data were not recorded at all flow ratios; therefore, in some cases, no arrows are indicated.

With few exceptions, the curves show a sharp dropoff in performance due to cavitation. No dropoff is indicated at some of the low-flow-ratio conditions. In these cases, the test facility lower limit of secondary inlet pressure, 9 feet (2.74 m) of water, was reached before cavitation was developed sufficiently to cause performance deterioration.

Effects of flow ratio. - The curves presented in figure 7 indicate that, for a fixed nozzle position, higher values of secondary inlet head $H_{s,v}$ were required to prevent total headrise deterioration as flow ratio was increased. This effect of flow ratio on the required net positive suction head is summarized in figure 8, a cross plot of figure 7. Although the required $H_{s,v}$ increased with increasing flow ratio, only 10 to 18 feet (3.05 to 5.5 m) of water were required at the best efficiency flow ratios ($M = 1.4$ for $R = 0.197$ and $M = 3.5$ for $R = 0.066$).

The principal reason for the increased susceptibility to cavitation at high flow ratios is evident from an analysis of the wall static pressure distributions in the test section. These distributions are presented in dimensionless form in figure 9 in terms of a pressure coefficient. The pressure coefficient is defined by

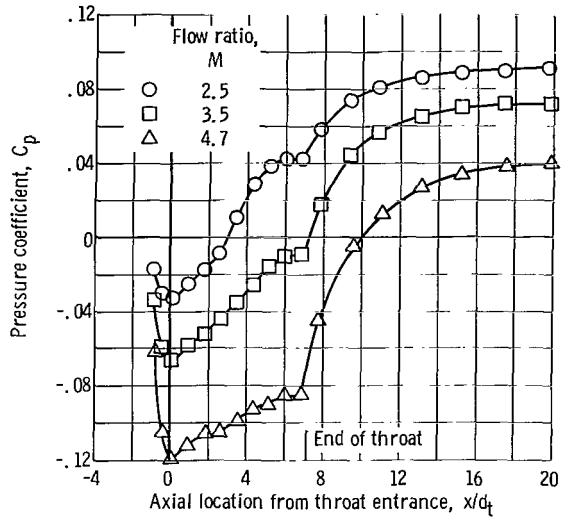

Figure 9. - Effect of flow ratio for nozzle spacing of zero and area ratio of 0.066.

$$C_p = \frac{p_x - p_2}{\frac{\gamma V_n^2}{2g}}$$

where the numerator represents the pressure rise above secondary inlet pressure at any axial location in the jet pump, and the denominator is the velocity head of the primary fluid at the nozzle exit.

At a given nozzle position, as flow ratio is increased, lower static pressures are measured in the secondary inlet and throat regions. Since the annular flow area is fixed, for a fixed nozzle position, an increase in flow ratio causes an increase in velocity and a corresponding decrease in static pressure. Also, the pressure gradient in the throat is comparatively small at high flow ratios. Fluid is exposed to low pressure over a longer period of time, and the tendency for increasing pressure to collapse the cavitation bubbles is reduced.

Effect of nozzle spacing. - Another prominent effect apparent from figure 7 is that cavitation performance improved as the nozzle was retracted. This effect is summarized in figure 10, a cross plot of figure 7. Less net positive suction head was required to prevent performance deterioration as the nozzle was retracted for both area ratios considered. The reasons for this can be ascertained from an examination of the wall static pressure distributions, for three nozzle spacings, presented in figure 11. For any fixed

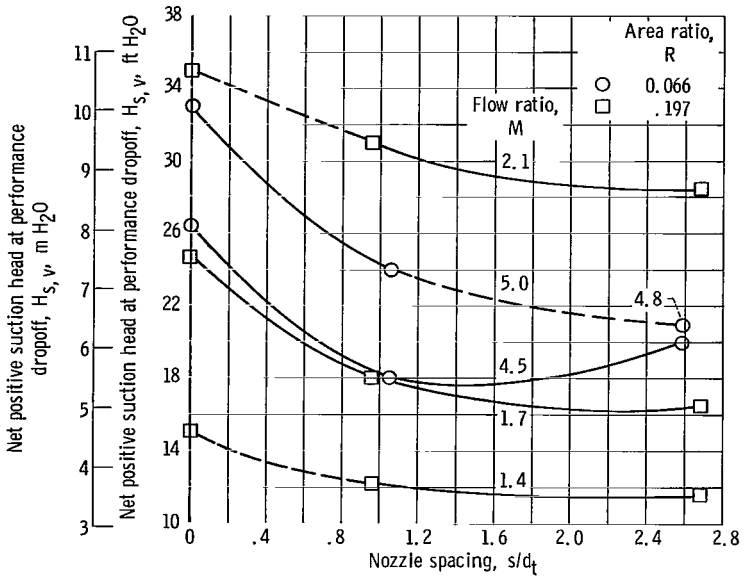

Figure 10. - Effect of nozzle spacing on required net positive suction head of secondary fluid.

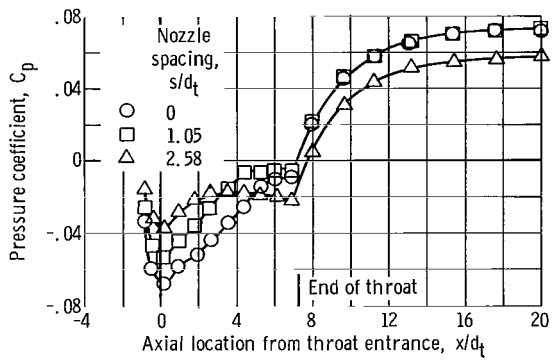

Figure 11. - Effect of nozzle spacing on static pressure distribution for flow ratio of 3.5 and area ratio of 0.066.

flow condition, it is apparent that, as nozzle spacing is reduced, the level of static pressure decreases. This decrease occurs because the annular flow area of the secondary fluid is reduced as the nozzle is moved closer to the throat inlet. An equal amount of flow passing through a smaller area produces higher velocities and lower static pressures.

Another factor, of secondary importance, also contributes to increased sensitivity to cavitation at small nozzle spacings. In the fully inserted position, the effect of a finite thickness of the nozzle wall at the exit becomes more prominent. In the present

investigation, practical machining requirements resulted in a finite thickness at the exit of each nozzle of 0.027 inch (0.069 cm) (see fig. 4). The fluid dynamic effect of the nozzle wall thickness is the creation of a wake which coincides in location with the shear layer between the two fluids. The wake acts to increase the turbulence level of the mixing layer, and therefore to increase susceptibility to cavitation. As the nozzle is retracted into the settling chamber, the effect of nozzle wall thickness is diminished because the static pressure at the nozzle exit plane is higher.

From an efficiency standpoint, the best nozzle spacings for both area ratios are those between 0 and 1 throat diameter (fig. 6). From a cavitation standpoint, however, nozzle spacings of 1 throat diameter or larger are preferable (fig. 10). If both maximum efficiency and cavitation resistance were design objectives, they could be satisfied by the selection of a nozzle spacing (s/d_t) of approximately 1.0. It should be recognized that this criterion is not universal; optimum nozzle spacing is dependent on throat length and secondary inlet configuration.

Photographs of cavitation. - Photographs of various stages of cavitation for both area ratios are shown in figure 12. The flow conditions depicted correspond to conditions plotted in figure 7. Visually, there was no significant effect of area ratio on the character of the cavitation. At the fully inserted nozzle position, visible incipient cavitation generally appeared first as isolated voids in midstream (fig. 12(a-1)), appearing and disappearing rapidly and randomly. Reductions in inlet pressure produced well-defined, sustained amounts of cavitation extending downstream from the exit plane of the nozzle (figs. 12(a-2), (a-5), (a-6), (b-2), (b-6), and (b-7)). Further reductions in inlet pressure caused the cavitating region to increase in downstream length and to spread radially outward to the wall (figs. 12(a-3), (a-4), (a-7), (a-8), (b-3), (b-4), and (b-9)). Substantial correlation appeared to exist between the point of performance dropoff and the condition for which the cavitation region contacted the wall. Generous amounts of cavitation could be tolerated before performance was affected.

The cavitation patterns depicted in figures 12(a-9) and (a-10) are typical of the forms of cavitation associated with nozzle spacings greater than zero. At large nozzle spacings (regardless of area ratio), the characteristics of the cavitation cloud were different from those associated with the fully inserted nozzle position. The cavitation cloud was relatively unstable, forming in explosive bursts well downstream of the nozzle exit. As inlet pressure was reduced, the cavitation cloud would frequently extend rapidly upstream and become "attached" to the nozzle. The phenomenon was quite random and not necessarily repeatable, whereas the cavitation patterns observed at the fully inserted nozzle position were comparatively steady and had a high degree of reproducibility.

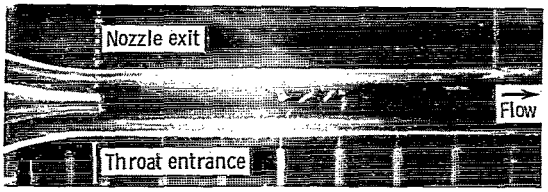

(a-1) Nozzle spacing, 0; flow ratio, 3.5; net positive suction head of secondary fluid, 26.1 feet (7.9 m); normalized head ratio, 1.0.

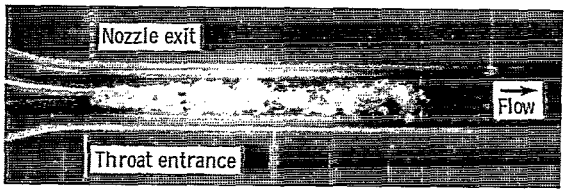

(a-2) Nozzle spacing, 0; flow ratio, 3.5; net positive suction head of secondary fluid, 18.5 feet (5.6 m); normalized head ratio, 1.0.

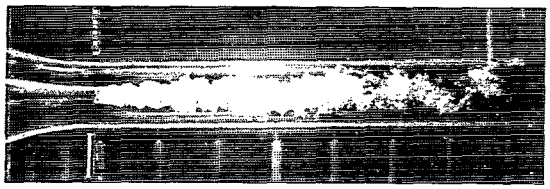

(a-3) Nozzle spacing, 0; flow ratio, 3.5; net positive suction head of secondary fluid, 17.6 feet (5.4 m); normalized head ratio, 1.0.

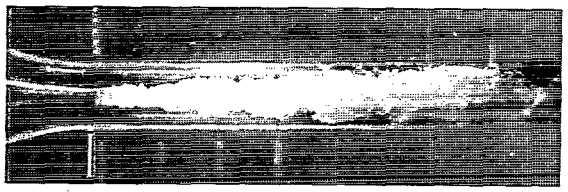

(a-4) Nozzle spacing, 0; flow ratio, 3.5; net positive suction head of secondary fluid, 15.6 feet (4.8 m); normalized head ratio, 1.0.

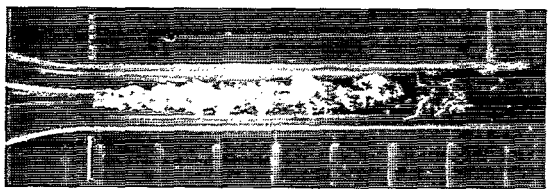

(a-5) Nozzle spacing, 0; flow ratio, 4.5; net positive suction head of secondary fluid, 30.8 feet (9.4 m); normalized head ratio, 1.0.

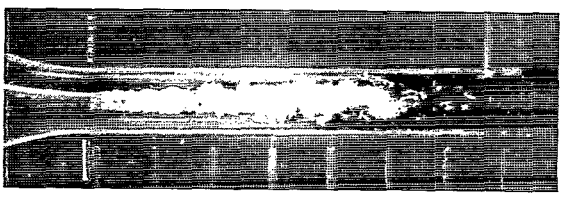

(a-6) Nozzle spacing, 0; flow ratio, 4.5; net positive suction head of secondary fluid, 28.4 feet (8.7 m); normalized head ratio, 0.97.

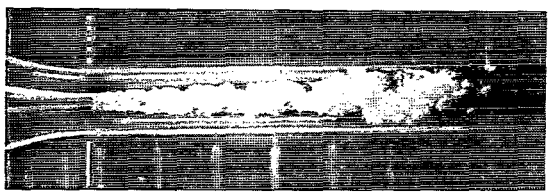

(a-7) Nozzle spacing, 0; flow ratio, 4.5; net positive suction head of secondary fluid, 26.8 feet (8.2 m); normalized head ratio, 0.97.

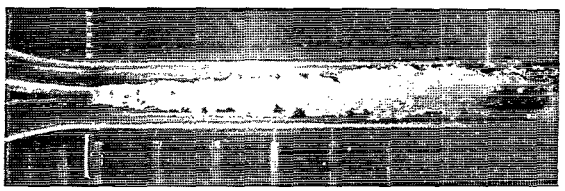

(a-8) Nozzle spacing, 0; flow ratio, 4.5; net positive suction head of secondary fluid, 25.7 feet (7.8 m); normalized head ratio, 0.51.

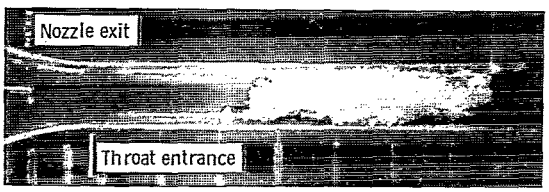

(a-9) Nozzle spacing, 1.05; flow ratio, 3.5; net positive suction head of secondary fluid, 10.9 feet (3.3 m); normalized head ratio, 0.99.

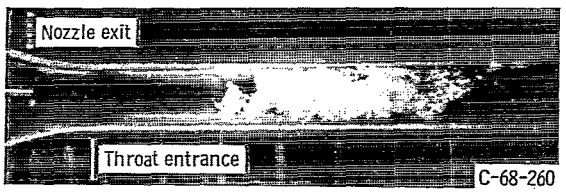

(a-10) Nozzle spacing, 1.05; flow ratio, 3.5; net positive suction head of secondary fluid, 10.1 feet (3.1 m); normalized head ratio, 0.98.

(a) Two nozzle positions; area ratio, 0.066.

Figure 12. - Development of cavitation as secondary inlet head is reduced.

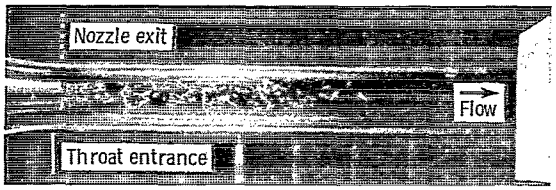

(b-1) Flow ratio, 1.3; net positive suction head of secondary fluid, 20.6 feet (6.3 m); normalized head ratio, 1.0.

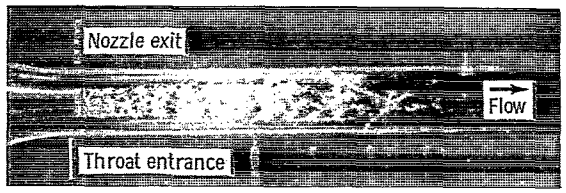

(b-2) Flow ratio, 1.3; net positive suction head of secondary fluid, 17.1 feet (5.2 m); normalized head ratio, 1.03.

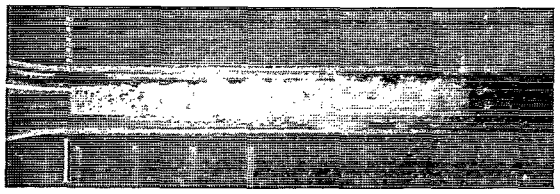

(b-3) Flow ratio, 1.3; net positive suction head of secondary fluid, 14.7 feet (4.5 m); normalized head ratio, 0.92.

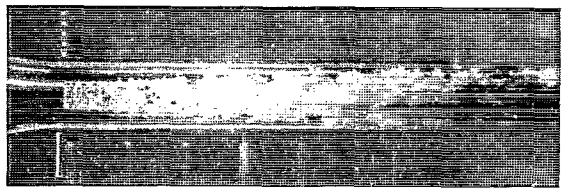

(b-4) Flow ratio, 1.3; net positive suction head of secondary fluid, 14.5 feet (4.4 m); normalized head ratio, 0.19.

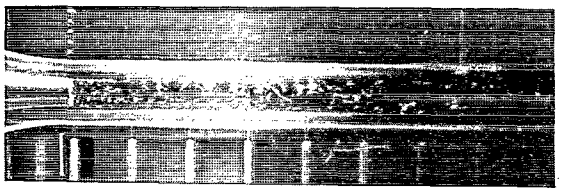

(b-5) Flow ratio, 2.0; net positive suction head of secondary fluid, 40.1 feet (12.2 m); normalized head ratio, 0.99.

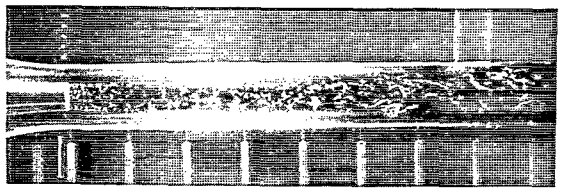

(b-6) Flow ratio, 2.0; net positive suction head of secondary fluid, 37.8 feet (11.5 m); normalized head ratio, 0.99.

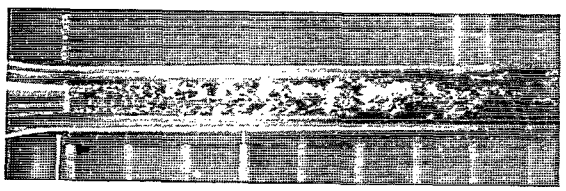

(b-7) Flow ratio, 2.0; net positive suction head of secondary fluid, 35.9 feet (10.9 m); normalized head ratio, 1.01.

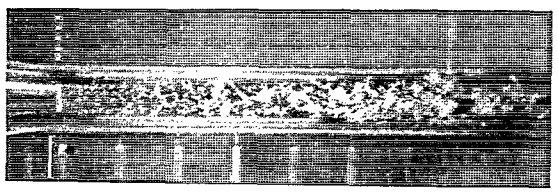

(b-8) Flow ratio, 2.0; net positive suction head of secondary fluid, 34.4 feet (10.5 m); normalized head ratio, 0.83.

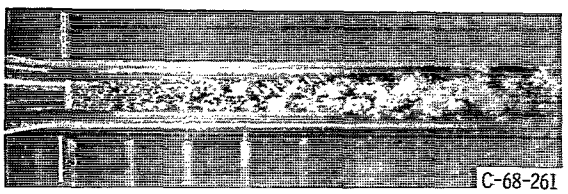

(b-9) Flow ratio, 2.0; net positive suction head of secondary fluid, 33.5 feet (10.2 m); normalized head ratio, 0.73.

(b) Fully inserted nozzle; area ratio, 0.197; nozzle spacing, 0.

Figure 12. - Concluded.

Prediction Parameters

Cavitation prediction parameter. - Several parameters which have been presented in the literature as jet flow or jet pump cavitation parameters were discussed earlier in the section MECHANISM AND ANALYSIS OF CAVITATION (p. 3). They are developed in appendix B sections I to III. It is then shown in appendix B section IV that these parameters are related, and that a prediction parameter ω can be derived from energy and continuity relations which correlates cavitation-caused total head dropoff points with the secondary- to primary-fluid velocity ratio V_3/V_n. This cavitation prediction parameter is defined as

$$\omega = \frac{P_2 - p_v}{\frac{\gamma V_n^2}{2g}} = \left(\frac{MR}{1 - R}\right)^2 (1 + K_s) = \left(\frac{V_3}{V_n}\right)^2 (1 + K_s) \tag{B7}$$

and is plotted as a function of velocity ratio in figure 13 for selected values of secondary inlet friction loss coefficient K_s.

The friction loss coefficients K are discussed in reference 3, and K_s is defined by

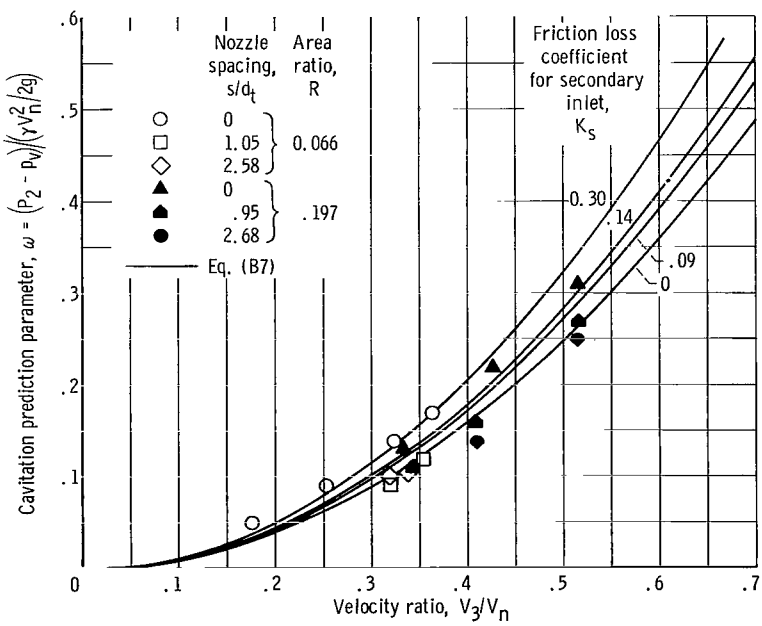

Figure 13. - Comparison of experimental and theoretical values of prediction parameter.

$$K_s = \frac{P_2 - P_3}{\frac{\gamma V_3^2}{2g}} \tag{B1}$$

Values of ω corresponding to points of performance dropoff are plotted in figure 13. Theoretical curves corresponding to several values of secondary friction loss coefficient are also plotted. The curves for $K_s = 0.09$ ($R = 0.066$) and $K_s = 0.14$ ($R = 0.197$) correspond to measured values of K_s as reported in reference 3. Also plotted for comparison purposes are curves that would correspond to secondary friction loss coefficients of 0 and 0.30.

It is apparent that, at the fully inserted nozzle position, the theory generally correlates the data, although the data fall slightly above the respective theoretical curves. This suggests that some factor not considered in the analysis had some influence on the cavitation process. As previously observed (Overall Cavitating Performance, Effect of nozzle spacing, p. 16), the wake produced by the primary nozzle walls increases the turbulence in the shear layer. The increase in turbulence intensifies the cavitation process and results in a premature deterioration in performance. The higher indicated values of ω for the smaller area ratio pump may be attributed to the larger relative size of the wake in that pump. Both nozzles had wall thicknesses of 0.027 inch (0.069 cm). This thickness represented about $4\frac{1}{2}$ percent of the nozzle internal diameter for $R = 0.197$ and 8 percent of the nozzle internal diameter for $R = 0.066$.

Effect of nozzle spacing: One of the premises of the analysis presented in appendix B section IV was that nozzle spacing is zero. It is therefore somewhat surprising that, for such a wide diversity of flows and area ratios, the values of ω for retracted nozzle positions agree so closely.

As discussed previously in the section Overall Cavitating Performance, Effect of nozzle spacing (p. 16), the effect of a retraction of the nozzle from the throat entrance is an increase of static pressure level in the secondary inlet region (with the consequent suppression of cavitation) and a reduction of the effect of nozzle wall thickness. Thus, as is evident from figure 13, retraction of the nozzle acts to reduce the effective value of ω. Although there is no method for predicting the effect quantitatively, an empirical value of $K_s = 0$ appears justified for predicting the cavitation dropoff conditions for nozzle spacings of $s/d_t \geq 1.0$.

At nozzle spacings less than 1 throat diameter, a value of K_s greater than the actual measured K_s may be necessary to account for the effect of nozzle wall thickness. The amount of "correction" in K_s that would be necessary would depend on the degree of departure from the zero wall thickness assumption.

Comparison with previously reported results: The theoretical curves for $K_s = 0$ and $K_s = 0.30$ are presented again in figure 14 together with a plot of the modified

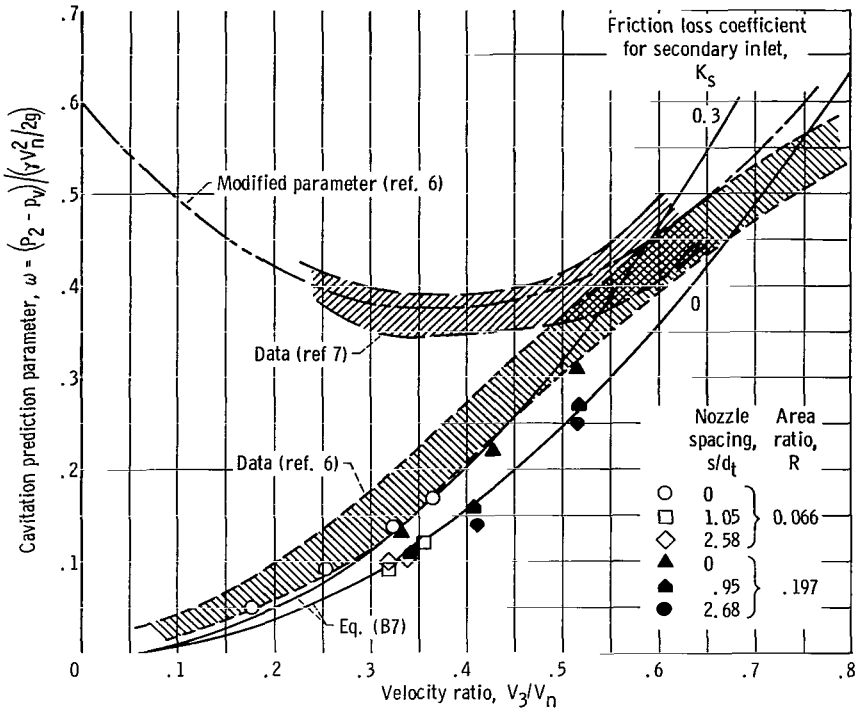

Figure 14. - Comparison of cavitation data from references 6 and 7 with prediction parameters from present report (eq. (B7)) and from reference 6.

Rouse parameter (appendix B section III), and data obtained by Mueller (ref. 7), Bonnington (ref. 6), and in this investigation. An examination of figure 14 reveals general agreement between Bonnington's data and the data obtained in the present investigation. There is, however, no agreement with the data reported by Mueller, except at velocity ratios greater than 0.5. It is not completely clear why the jet pumps tested by Mueller cavitated at higher values of ω. But it appears that the performance dropoff was abnormally early and may be related to blockage of the secondary flow area by the primary nozzle external contour. A drawing of the primary nozzle in position in one of the two secondary inlets tested is reproduced from reference 7 in figure 15. The exterior contour of nozzle A creates a converging-diverging secondary inlet area, presenting a greater-than-normal restriction to the secondary flow. Although the nozzle spacing or spacings at which Mueller's cavitation data were taken are not noted specifically in reference 7, numerical examples cited by the author use $s = 0.022$ inch (0.056 cm). At that nozzle position, a calibration of the secondary inlet region (ref. 7) had indicated extremely high losses ($K_s \sim 0.73$). It should therefore not be unexpected that Mueller's pumps exhibited a high susceptibility to cavitation. The apparent correlation between the Mueller data and

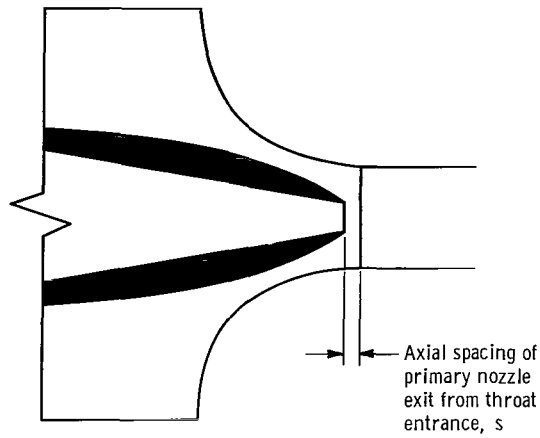

Figure 15. - Schematic drawing of primary nozzle and secondary inlet contours used in cavitation tests of reference 7.

Bonnington's modification of the Rouse parameter may only have been coincidental, the direct result of a restricted inlet region. Considering this, and the correlation of the Bonnington data and the data of this investigation with the ω parameter (eq. (7)), it may logically be concluded that ω is the more valid jet pump prediction parameter.

It should be quite clear from the foregoing discussion that the external contour of the primary nozzle and the contour of the secondary inlet region are extremely important design parameters. Proper hydrodynamic streamlining will produce lower losses and therefore improved noncavitating performance levels. But, more important, in order to prevent premature cavitation, the secondary flow passage should be smooth and unrestricted, and the nozzle wall thickness should be minimized.

Alternate cavitation prediction parameter. - In appendix B section V, an alternate cavitation parameter α is developed (eq. (B8)) which eliminates the need to express cavitation results as a function of velocity ratio. With α defined as

$$\alpha = \frac{P_2 - p_v}{\frac{\gamma V_3^2}{2g}}$$

at the condition of cavitation-induced total headrise dropoff, the one-dimensional application of the energy equations predicts

$$\alpha = 1 + K_s \tag{B8}$$

Therefore, the value of α at which the break in performance occurs should correspond to 1.0 plus the value of the secondary inlet friction loss coefficient K_s.

The same data presented in figure 13 were expressed in terms of α and presented in figure 16. The ordinate is a ratio of operating head ratio N to the noncavitating value of head ratio N_{NC} at the specified flow conditions, and the parameter α is expressed as the abscissa. Reduction of net positive suction head of the secondary fluid corresponds to a reduction of α. Therefore, figure 16 may be considered to be analogous to a conventional pump headrise as a function of the net positive suction head characteristic.

With few exceptions, performance dropped off at nearly the same values of α for a specific nozzle position. In some cases curved characteristics resulted after dropoff began (i.e., α increased as performance deteriorated). This was caused by difficulties in maintaining flow ratio constant after performance degradation had begun. Regardless

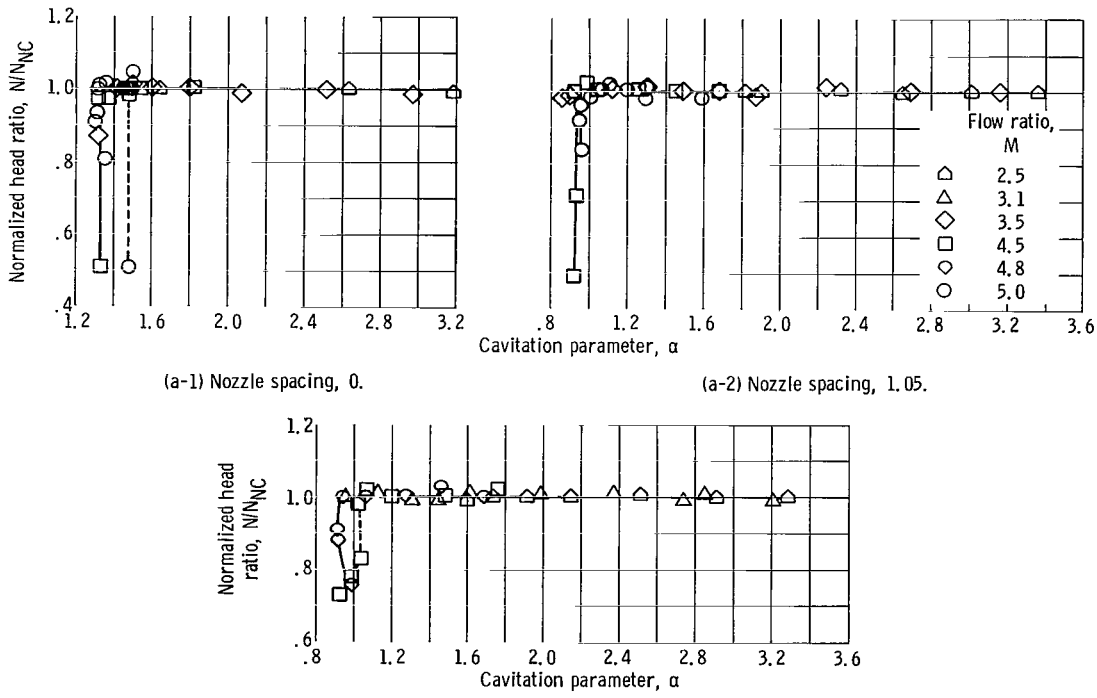

(a-1) Nozzle spacing, 0.

(a-2) Nozzle spacing, 1.05.

(a-3) Nozzle spacing, 2.58.

(a) Area ratio, 0.066; primary flow rate, 33.0 gallons per minute (2.08×10^{-3} m^3/sec).

Figure 16. - Jet pump cavitation performance as function of cavitation parameter.

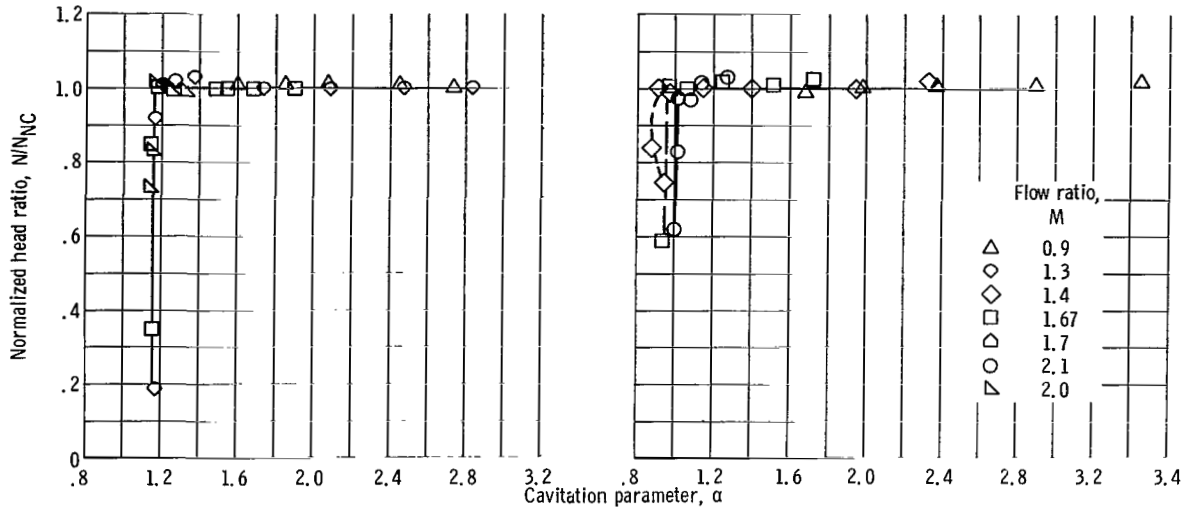

(b-1) Nozzle spacing, 0.

(b-2) Nozzle spacing, 0.95.

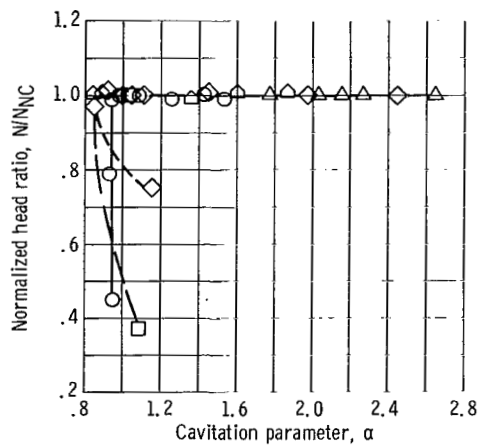

(b-3) Nozzle spacing, 2.68.

(b) Area ratio, 0.197; primary flow rate, 75.0 gallons per minute (4.74×10^{-3} m^3/sec).

Figure 16. - Concluded.

of area ratio or flow ratio, performance dropped off at values of α between 0.9 and 1.0 at moderate to large nozzle spacings ($s/d_t > 1.0$). For fully inserted nozzle positions, the values of α at performance dropoff were 1.17 for $R = 0.197$ and 1.32 for $R = 0.066$. The values of K_s inferred from figure 16 are identical to the values inferred from figure 13 (ω against V_3/V_n). This is not unexpected because $\omega = \alpha(V_3/V_n)^2$.

SUMMARY OF RESULTS

The cavitation performance of two jet pumps having nozzle- to throat-area ratios of

0.066 and 0.197 was evaluated in a closed loop facility using room-temperature, deaerated water. Each of the two nozzles was operated at three spacings of the nozzle exit upstream from the throat entrance.

The investigation yielded the following principal results:

1. Two related cavitation dropoff prediction parameters are presented which correlated the experimental data with reasonable accuracy. For both parameters, it was necessary to use an empirical loss coefficient for nozzle spacings between 0 and 1 throat diameter. It was possible to neglect this coefficient at larger nozzle spacings.

2. At any fixed nozzle position, higher net-positive-suction head of the secondary fluid was required to suppress cavitation as secondary- to primary-flow ratio was increased.

3. At any fixed flow ratio, less net-positive-suction head of the secondary fluid was required to suppress cavitation as the nozzle was retracted from the throat inlet. At nozzle spacings greater than or equal to approximately 1 throat diameter, the cavitation cloud was rather unstable, whereas the cavitation patterns observed at zero nozzle spacing were comparatively steady and had a high degree of reproducibility.

4. Both high efficiency and cavitation resistance were achieved at a nozzle spacing of 1 throat diameter from the throat entrance for the test pump configurations evaluated in this investigation.

5. The design of the secondary inlet region, which includes the exterior contour of the primary nozzle, is critical to jet pump cavitation performance. The secondary fluid annular flow path, as described by the secondary inlet contour and the primary nozzle exterior contour, should be hydrodynamically streamlined and smoothly converging to the throat entrance. The primary nozzle wall thickness should be as thin as possible.

6. As net positive suction head of the secondary fluid was decreased, generous amounts of cavitation were tolerated in the mixing chamber before efficiency and head ratio deteriorated. However, when performance did deteriorate it did so quite sharply.

Lewis Research Center,
National Aeronautics and Space Administration,
Cleveland, Ohio, December 13, 1967,
128-31-06-28-22.

APPENDIX A

SYMBOLS

A	area, ft^2; m^2
C_p	pressure coefficient, $(p_x - p_2)/\left[\gamma(V_n^2/2g)\right]$
c	dimensional constant, 448.9 (gal/min)/(ft^3/sec)
d	diameter, in.; cm
g	acceleration due to gravity, 32.163 ft/sec^2; 9.803 m/sec^2
g_c	dimensional constant, 32.174(ft-lb mass)/(sec^2)(lb force); $\left[1.0\ (m\text{-}kg)/(sec^2\text{-}N)\right]$
H	total head of fluid, P/γ, ft; m
$H_{s,v}$	net positive suction head of secondary fluid, $(P_2 - p_v)/\gamma$, ft; m
K	friction loss coefficient
L	length, in.; cm
l	throat length, in.; cm
M	flow ratio, Q_2/Q_1
N	head ratio, $(H_5 - H_2)/(H_1 - H_5)$
N/N_{NC}	normalized head ratio; ratio of operating head ratio to noncaviting head ratio
P	total pressure, lb force/ft^2; N/m^2
p	static pressure, lb force/ft^2; N/m^2
p_v	vapor pressure, lb force/ft^2; N/m^2
Q	volumetric flow rate, gal/min; m^3/sec
R	area ratio, A_n/A_t
s	axial spacing of primary nozzle exit from throat entrance, in.; cm
V	velocity, ft/sec; m/sec
w	mass flow rate, lb mass/sec; kg/sec
x	linear distance measured in axial direction from throat entrance, in.; cm
α	jet pump cavitation prediction parameter at total headrise dropoff, $(P_2 - p_v)/\left[\gamma(V_3^2/2g)\right]$
β	diffuser included angle, deg; rad
γ	specific weight, $\rho(g/g_c)$, lb force/ft^3; N/m^3

η efficiency, MN

ρ fluid density, lb mass/ft^3; kg/m^3

σ_B jet pump cavitation prediction parameter (Bonnington) at total headrise dropoff,

$$\frac{\dfrac{P_2 - p_v}{\gamma \dfrac{V_n^2}{2g}} - \left(\dfrac{V_3}{V_n}\right)^2}{\left(1 - \dfrac{V_3}{V_n}\right)^2}$$

σ_R free jet incipient cavitation prediction parameter (Rouse), $(p_F - p_v)/\left[\gamma(V_o^2/2g)\right]$

ω jet pump cavitation prediction parameter at total headrise dropoff, $(P_2 - p_v)/\left[\gamma(V_n^2/2g)\right]$

Subscripts:

bep best efficiency point

d diffuser

F ambient fluid, free jet

f friction

n primary nozzle exit plane, jet pump

o nozzle exit plane, free jet

p primary nozzle

s secondary fluid inlet

t throat

ts test section

x linear position measured in axial direction from throat entrance

1 primary fluid

2 secondary fluid

3 location at throat entrance

4 location at throat exit

5 location at jet pump discharge

APPENDIX B

DEVELOPMENT OF JET PUMP CAVITATION ANALYSES

The jet pump analyses presented to date share certain common assumptions:

(1) Both the primary and secondary fluids are incompressible.

(2) The temperatures of the primary and secondary fluids are equal.

(3) Spacing of the nozzle exit from the throat entrance is zero ($s/d_t = 0$).

(4) The primary nozzle wall thickness at the exit is zero ($A_3 = A_t - A_n$).

(5) At the point of total headrise dropoff, the static pressure in the throat entrance plane p_3 is equivalent to the vapor pressure of the secondary fluid.

Presented in the following sections are three analyses and the resultant parameters which have been important in the development of jet pump cavitation prediction routines. Two additional parameters are then derived which are related to the previous three.

I. Gosline and O'Brien Analysis

Gosline and O'Brien (ref. 4) applied the one-dimensional energy and continuity relations to the secondary fluid and accounted for friction through the use of a dimensionless friction loss coefficient K_s (ref. 3). The nomenclature used in the following equations was established in figures 1 and 17.

$$\frac{p_2}{\gamma} + \frac{V_2^2}{2g} = \frac{p_3}{\gamma} + \frac{V_3^2}{2g} + \frac{\Delta P_{f,s}}{\gamma}$$

$$\frac{P_2}{\gamma} = \frac{p_3}{\gamma} + \frac{V_3^2}{2g}(1 + K_s)$$

where

$$K_s = \frac{\Delta P_{f,s}}{\gamma \frac{V_3^2}{2g}} = \frac{P_2 - P_3}{\gamma \frac{V_3^2}{2g}} \tag{B1}$$

$$P_2 - p_3 = \gamma \frac{V_3^2}{2g}(1 + K_s) \tag{B2}$$

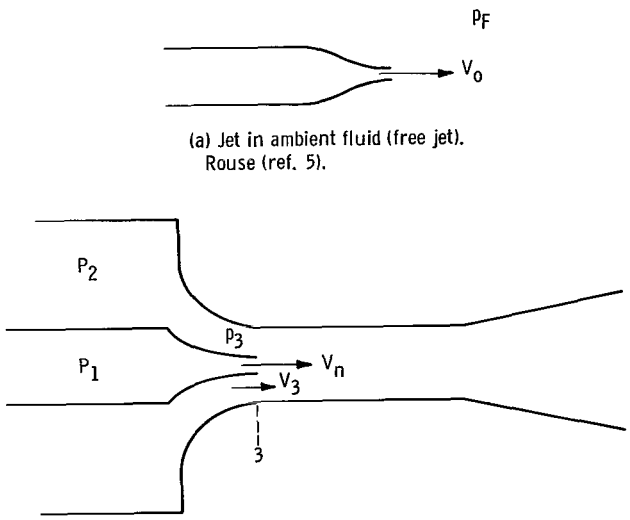

(a) Jet in ambient fluid (free jet). Rouse (ref. 5).

(b) Jet pump flow (ducted jet).

Figure 17. - Comparison of nomenclature for free jet and ducted jet.

$$V_3 = \sqrt{\frac{P_2 - p_3}{\frac{\gamma}{2g}(1 + K_s)}}$$

$$Q_2 = cA_3\sqrt{\frac{P_2 - p_3}{\frac{\gamma}{2g}(1 + K_s)}}$$

where

$$A_3 = A_t - A_n$$

At the point of total headrise dropoff due to cavitation, it is assumed that static pressure in the exit plane of the nozzle p_3 is reduced to its lower limit, that is, vapor pressure p_v. Therefore,

$$Q_2 = cA_3\sqrt{\frac{P_2 - p_v}{\frac{\gamma}{2g}(1 + K_s)}} \tag{B3}$$

at the point of total headrise dropoff. The value of Q_2 that is calculated from equation (B3) is the limiting value of secondary flow as determined by cavitation.

II. Rouse Parameter

Rouse (ref. 5) utilized a cavitation parameter to correlate incipient cavitation data for a free jet (refer to fig. 17(a)). The parameter is conventionally defined as

$$\sigma_R = \frac{p_F - p_v}{\gamma \frac{V_o^2}{2g}} \tag{B4}$$

He observed incipient cavitation to occur at values of $\sigma_R = 0.6$.

III. Bonnington Modified Rouse Parameter

Bonnington attempted to modify Rouse's free jet parameter to apply to ducted jets, the case of interest for jet pump flow (ref. 6). In his analysis, he neglected the vapor pressure term in Rouse's parameter, apparently because of its relative insignificance in cold water. It shall be retained here. The following modifications to equation (4) were made by Bonnington (refer to fig. 17(b)):

(1) p_F corresponds to p_3

(2) V_o corresponds to V_n, but the denominator $\gamma(V_o^2/2g)$ corresponds to $\gamma(V_n - V_3)^2/2g$ because in a free jet the velocity of the entrained fluid V_3 is zero, whereas in a ducted jet it has a finite value

Therefore,

$$\sigma_B = \frac{p_3 - p_v}{\frac{\gamma(V_n - V_3)^2}{2g}} \tag{B5}$$

When friction is neglected,

$$p_3 = P_2 - \frac{\gamma V_3^2}{2g}$$

$$\sigma_B = \frac{(P_2 - p_v) - \dfrac{\gamma V_3^2}{2g}}{\dfrac{\gamma (V_n - V_3)^2}{2g}}$$

Divide the numerator and the denominator by $\gamma(V_n^2/2g)$:

$$\sigma_B = \frac{\dfrac{P_2 - p_v}{\dfrac{\gamma V_n^2}{2g}} - \left(\dfrac{V_3}{V_n}\right)^2}{\left(1 - \dfrac{V_3}{V_n}\right)^2}$$

Rouse found incipient cavitation to occur when $\sigma_R = 0.6$. Bonnington assumed total head breakdown in a jet pump to occur also at a value of 0.6. Setting $\sigma_B = 0.6$ and solving for $(P_2 - p_v)/\left[(\gamma/2g)\, V_n^2\right]$ leads to

$$\frac{P_2 - p_v}{\dfrac{\gamma}{2g} V_n^2} = 0.6 - 1.2\,\frac{V_3}{V_n} + 1.6\left(\frac{V_3}{V_n}\right)^2 \tag{B6}$$

This equation is presented graphically in figure 14 as the modified parameter.

IV. Cavitation Prediction Parameter

The parameter proposed in this section is derived in a manner quite similar to the Gosline and O'Brien approach. The energy equation applied to the secondary fluid results in

$$P_2 - p_3 = \frac{\gamma V_3^2}{2g}(1 + K_s) \tag{B2}$$

Divide each side by $\gamma(V_n^2)/2g$:

$$\frac{P_2 - p_3}{\frac{\gamma V_n^2}{2g}} = \left(\frac{V_3}{V_n}\right)^2 (1 + K_s)$$

Define

$$\omega = \frac{P_2 - p_3}{\frac{\gamma V_n^2}{2g}}$$

For the fully inserted nozzle position $s/d_t = 0$ and a nozzle wall thickness of zero,

$$\frac{V_3}{V_n} = \frac{Q_2}{A_3}\frac{A_n}{Q_1} = M\frac{A_n}{A_t - A_n}$$

$$\frac{V_3}{V_n} = \frac{MR}{1 - R}$$

Thus,

$$\omega = \frac{P_2 - p_3}{\frac{\gamma V_n^2}{2g}} = \left(\frac{V_3}{V_n}\right)^2 (1 + K_s) = \left(\frac{MR}{1 - R}\right)^2 (1 + K_s)$$

If it is assumed that, at cavitation dropoff $p_3 = p_v$, the parameter ω becomes

$$\omega = \frac{P_2 - p_v}{\frac{\gamma V_n^2}{2g}} = \left(\frac{MR}{1 - R}\right)^2 (1 + K_s) = \left(\frac{V_3}{V_n}\right)^2 (1 + K_s) \tag{B7}$$

at the point of total headrise dropoff.

V. Alternate Cavitation Prediction Parameter

Beginning identically to the development of ω,

$$P_2 - p_3 = \frac{\gamma V_3^2}{2g}(1 + K_s) \tag{B2}$$

Divide each side by $\gamma V_3^2/2g$:

$$\frac{P_2 - p_3}{\frac{\gamma V_3^2}{2g}} = 1 + K_s$$

Define

$$\alpha = \frac{P_2 - p_3}{\frac{\gamma V_3^2}{2g}}$$

If $p_3 = p_v$ at total headrise dropoff conditions,

$$\alpha = \frac{P_2 - p_v}{\frac{\gamma V_3^2}{2g}} = (1 + K_s) \tag{B8}$$

at the point of total headrise dropoff. It should be noted that $\omega = \alpha(V_3/V_n)^2$. Both ω and $\underline{\alpha}$ are directly related to the approach presented by Gosline and O'Brien (ref. 4).

REFERENCES

1. Sanders, Newell D.; Barrett, Charles A.; Bernatowicz, Daniel T.; Moffitt, Thomas P.; Potter, Andrew E., Jr.; and Schwartz, Harvey J.: Power for Spacecraft. Proceedings of the NASA-University Conference on the Science and Technology of Space Exploration. Vol. 2. NASA SP-11, 1962, pp. 125-150.
2. Chalpin, E. S.; Pope, J. R.; and Foss, C. L.: Development of a SNAP-8 Pump for Mercury Service. AIAA Specialists Conference on Rankine Space Power Systems. Vol. I. AEC Rep. No. CONF-651026. Vol. 1, pp. 171-185.
3. Sanger, Nelson L.: Noncavitating Performance of Two Low-Area-Ratio Water Jet Pumps Having Throat Lengths of 7.25 Diameters. NASA TN D-4445, 1968.
4. Gosline, James E. and O'Brien, Morrough P.: The Water Jet Pump. Univ. California Publ. Eng., vol. 3, no. 3, 1933, pp. 167-190.
5. Rouse, Hunter: Cavitation in the Mixing Zone of a Submerged Jet. LaHouille Blanche, vol. 8, Jan.-Feb. 1953, pp. 9-19.
6. Bonnington, S. T.: The Cavitation Limits of a Liquid-Liquid Jet Pump. Publ. RR-605, British Hydromechanics Research Assoc., Harlow, Essex, England, 1958.
7. Mueller, N. H. G.: Water Jet Pump. Proc. Am. Soc. Civil Eng., J. Hydraulics Div., vol. 90, no. HY3, May 1964, pp. 83-113.
8. Schulz, F.; and Fasol, K. H.: Wasserstrahlpumpen zur Förderung von Flüssegkeiten. Springer Verlag, Vienna, 1958.
9. Vogel, R.: Theoretische und Experimentelle Unterschungen as Strahlapparaten. Maschinenbautechnik, Berlin, vol. 5, 1956, pp. 619-637.
10. Holl, J. William; and Wislicenus, George F.: Scale Effects on Cavitation. J. Basic Eng., vol. 83, no. 3, Sept. 1961, pp. 385-398.
11. Eisenberg, Phillip: Mechanics of Cavitation. Handbook of Fluid Dynamics. Victor L. Streeter, ed., McGraw-Hill Book Co., Inc., 1961, pp. 12-2 to 12-9.
12. Frenkel, J.: Kinetic Theory of Liquids. Clarendon Press, Oxford, 1946.
13. Blake, F. G., Jr.: The Onset of Cavitation in Liquids. Tech. Rep. No. 12, Acoustics Research Lab., Harvard Univ., Sept. 1949.
14. Knapp, Robert T.: Investigation of the Mechanics of Cavitation and Cavitation Damage. Final Rep., Hydrodynamics Lab., California Inst. Tech. (Contract NONR-22008), June 1957.

15. Parkin, B. R.; and Kermeem, R. W.: Incipient Cavitation and Boundary Layer Interaction on a Streamlined Body. Rep. No. E-35.2, Hydrodynamics Lab., California Inst. Tech., Dec. 1953.

16. Williams, E. E.; and McNulty, P.: Some Factors Affecting the Inception of Cavitation. Cavitation in Hydrodynamics, National Physical Lab., Great Britain, Sept. 14-17, 1955.

17. Eisenberg, Phillip: Cavitation. Intern. Sci. Tech., no. 14, Feb. 1963, pp. 72-76, 79-80, 82, 84.

18. Daily, J. W.; and Johnson, V. E., Jr.: Turbulence and Boundary-Layer Effects on Cavitation Inception from Gas Nuclei. Trans. ASME, vol. 78, no. 8, Nov. 1956, pp. 1695-1706.

19. Holl, J. William; and Treaster, A. L.: Cavitation Hysteresis. J. Basic Eng., vol. 88, no. 1, Mar. 1966, pp. 199-212.

20. Lienhard, J. H.; and Stephenson, J. M.: Temperature and Scale Effects Upon Cavitation and Flashing in Free and Submerged Jets. J. Basic Eng., vol. 88, no. 2, June 1966, pp. 525-532.

NATIONAL AERONAUTICS AND SPACE ADMINISTRATION
WASHINGTON, D. C. 20546

OFFICIAL BUSINESS

FIRST CLASS MAIL

POSTAGE AND FEES PAID
NATIONAL AERONAUTICS AND
SPACE ADMINISTRATION

C6L C01 53 51 3DS 68134 00903
AIR FORCE WEAPONS LABORATORY/AFWL/
KIRTLAND AIR FORCE BASE, NEW MEXICO 8711

ATT MISS MADELINE F. CANOVA, CHIEF TECHN
LIBRARY /WLIL/

POSTMASTER: If Undeliverable (Section 158 Postal Manual) Do Not Return

"The aeronautical and space activities of the United States shall be conducted so as to contribute . . . to the expansion of human knowledge of phenomena in the atmosphere and space. The Administration shall provide for the widest practicable and appropriate dissemination of information concerning its activities and the results thereof."

— NATIONAL AERONAUTICS AND SPACE ACT OF 1958

NASA SCIENTIFIC AND TECHNICAL PUBLICATIONS

TECHNICAL REPORTS: Scientific and technical information considered important, complete, and a lasting contribution to existing knowledge.

TECHNICAL NOTES: Information less broad in scope but nevertheless of importance as a contribution to existing knowledge.

TECHNICAL MEMORANDUMS: Information receiving limited distribution because of preliminary data, security classification, or other reasons.

CONTRACTOR REPORTS: Scientific and technical information generated under a NASA contract or grant and considered an important contribution to existing knowledge.

TECHNICAL TRANSLATIONS: Information published in a foreign language considered to merit NASA distribution in English.

SPECIAL PUBLICATIONS: Information derived from or of value to NASA activities. Publications include conference proceedings, monographs, data compilations, handbooks, sourcebooks, and special bibliographies.

TECHNOLOGY UTILIZATION PUBLICATIONS: Information on technology used by NASA that may be of particular interest in commercial and other non-aerospace applications. Publications include Tech Briefs, Technology Utilization Reports and Notes, and Technology Surveys.

Details on the availability of these publications may be obtained from:

SCIENTIFIC AND TECHNICAL INFORMATION DIVISION

NATIONAL AERONAUTICS AND SPACE ADMINISTRATION

Washington, D.C. 20546